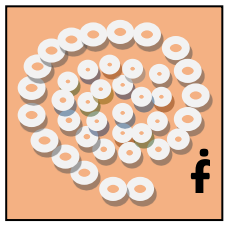

International Journal of Mathematical Analysis and Modelling

(Formerly Journal of the Nigerian Society for Mathematical Biology)

Volume 7 Issue 2, 2024

ISSN (Print): 2682 - 5694
ISSN (Online): 2682 – 5708
www.tnsmb.org

Mathematical fractional model for the dynamics and control of Diphtheria transmission

E. Abah[*], B. Bolaji[†], W. Atokolo[‡§], G.O. Acheneje[¶], B.I. Omede[‖], J. Amos[*,**] and D. Omeje[††]

Abstract

Diphtheria is an acute bacterial infection primarily affecting the upper respiratory tract, caused by Corynebacterium diphtheriae. This study uses a fractional-order mathematical model to assess the effects of therapy and vaccination on diphtheria transmission dynamics. Initially, the model employs integer-order nonlinear differential equations with minimal vaccination and treatment. To better understand disease dynamics, it is then adapted with fractional-order derivatives and power laws. The research includes a stability analysis of the endemic equilibrium using the Lyapunov function approach and establishes conditions for the existence and uniqueness of solutions in the fractional-order model. To explore factors influencing disease spread, a sensitivity analysis of the basic reproduction number was conducted. Numerical simulations using the fractional Adams–Bashforth–Moulton method offer insights into how model parameters and fractional-order values impact diphtheria dynamics and control. Additional simulations with surface and contour plots revealed that higher contact rates and lower vaccine efficiency would increase diphtheria prevalence. Conversely, improving treatment and immunization programs is expected to reduce the incidence of diphtheria in the general population.

Keywords and phrases: Diphtheria; fractional; Adam-Bashforth-Moulton; transmission

1 Introduction

Exotoxins produced by Corynebacterium bacteria, which cause diphtheria, are known to cause damage to human tissue [1]. Hippocrates, in the fifth century BC, is the first recorded mention of this illness, which has afflicted humans for ages. For a long time, diphtheria has been a leading cause of infant mortality and a devastating menace in both industrialized and developing countries [2]. Many individuals in contemporary and emerging nations are still susceptible to diphtheria despite extensive immunization [3]. The disease is endemic in a number of places, including Brazil, the tropics, South America, Africa, and India, even in locations with high exposure over a period of five to ten years, as recorded cases continue to occur[4],[5],[6]. In the Russian Federation, diphtheria has been on the rise since the early 1990s and has spread to all of the Newly Independent States (NIS). Between 64 Percent

[*]E-mail: abahemmanuel1995@gmail.com; Department of Mathematics Sciences, Prince Abubakar Audu University, Anyiba, Nigeria

[†]Department of Mathematics Sciences, Prince Abubakar Audu University, Anyigba, Nigeria; E-mail: bolarinwa.s.bolaji@gmail.com

[‡]Corresponding Author; E-mail: williamsatokolo@gmail.com

[§]Department of Mathematics Sciences, Prince Abubakar Audu University, Anyigba, Nigeria

[¶]Department of Mathematics Sciences, Prince Abubakar Audu University, Anyigba, Nigeria; E-mail: achenejegodwin@gmail.com

[‖]Department of Mathematics Sciences, Prince Abubakar Audu University, Anyigba, Nigeria; E-mail: benjaminomede197@gmail.com

[**]Department of Mathematics Sciences, Prince Abubakar Audu University, Anyigba, Nigeria; E-mail: amosjeremiah1997@gmail.com

[††]Department of Mathematics Sciences, Prince Abubakar Audu University, Anyigba, Nigeria; E-mail: omejedaniel3269@gmail.com

and 82 percent of people over the age of 15 contract diphtheria each year; by 1999, this had resulted in a considerable number of cases and fatalities. Nearly half of all deaths in several nations occur in individuals between the ages of 40 and 49, who are disproportionately impacted; cases in adults over 50 are less common [3]. The bacteria readily attach themselves to the tissue in the throat, releasing exotoxins that eventually cause a pseudo membrane to form [7],[8]. The initial set of symptoms resembles those of the flu, but they also include fever, swollen lymph nodes, coughing, hoarseness, and shortness of breath. Additionally, some patients may have skin involvement that leads to skin ulcers. Ill health and compromised respiratory defenses increase the severity of diphtheria [9]. The study of mathematical epidemiology has made significant contributions to our understanding of the dynamics of infectious illnesses, their effects, and potential future spread forecasts. Different prevention, detection, control, and rehabilitation programs are compared, evaluated, planned, implemented, and optimized using mathematical models.

To help medical professionals reduce the disease loads of infectious diseases within any community, a variety of mathematical models have been developed by various authors. When studying and examining the dynamics of infectious disease transmission within a population, these models are a priceless resource. For example, Atokolo et al [10] formulated strategies for limiting the Zikavirus's propagation and investigated the fractional order sterile insect technology (SIT) paradigm. The model's analytical solution was created using the Laplace–Adomian decomposition method (LADM), and it perfectly converges to the right value. The response behaviors of the model are more flexible due to its fractional order structure. The report notes that, to the best of current knowledge, this is the first instance of using LADM to solve a SIT model. In order to investigate the epidemiology of Lassa fever, Atokolo et al. [11] combined integer-order nonlinear differential equations with fractional-order derivatives to create a fractional-order mathematical model that allowed them to analyze the dynamics of the illness. Numerical simulations indicate that lower vaccine effectiveness and greater contact rates are positively correlated with the prevalence of Lassa disease. Improving vaccination and treatment plans may help lower this incidence, the report suggests. A stability analysis of the endemic equilibrium is also included in the work. Agahiu et al. [12] offered a mathematical model designed to comprehend the dynamics of the co-infections of the Zika and Chikungunya viruses. The model uses the Laplace Adomians Decomposition Method (LADM) to account for the intricate interactions that take place between human populations and sick insects. Numerical models demonstrate that increasing bed net usage and decreasing mosquito biting rates might significantly control the dynamics of Zika-Chikungunya co-infections in Espirito Santo State, Brazil. Odionyenma et al. [13] provided a fractional derivative model that analyzes the dynamics of the co-infection between Chlamydia and Gonorrhea while ensuring positivity boundedness and uniqueness using the Laplace transform and fixed point theorems. It demonstrates Ulam-Hyers-Rassias stability in comparison to conventional integer-order models, indicating its robustness in accurately and realistically describing the dynamics of Chlamydia-Gonorrhea co-infection. Zhang et al. [14] offered a novel mathematical model for analyzing the COVID-19 pandemic that takes into account five distinct categories: susceptible, exposed, infected, isolated, and recovered people. Using the adaptive predictor-corrector algorithm and the fourth-order Runge-Kutta method, the paper investigates the numerical approximations and dynamics of the model, addressing themes such as positivity, boundedness, basic reproduction number calculation, asymptotic stability, and simulation methodologies. The theoretical conclusions are corroborated by the study's numerical simulations. Ghani et al. [15] offered a fractional mathematical model with variables for innate immunity, treatment, and vaccination for studying diphtheria. The model consists of five compartments: exposed, infected, isolated, recovered, and vulnerable individuals. Analytical proofs are provided for the model's well-posedness, stability characteristics, and predictor-corrector scheme. Numerical simulations are validated using the least squares method, and results are reported that are comparable across different fractional orders. Mangal et al. [16] studied how vaccination campaigns and booster doses affect highly contagious diseases using a fractional-order epidemic model. It looks into stability analysis, Hopf bifurcation occurrences, and the dynamics of disease transmission. The research concludes that awareness programs are a more effective strategy to reduce outbreaks than booster immunizations,

after validating the model with real COVID-19 patient data from Canada and Norway. Rajan et al. [17] used a fractional modeling method to investigate the dynamics of HPV transmission and the connection between HPV and cervical cancer. Compartmental modeling is utilized to identify vulnerable, infected, and recovered populations. The model incorporates a Caputo fractional derivative to account for the development of non-local illnesses and long-term memory effects. The Banach fixed point theorem, Lyapunov functions, and numerical simulations are used in the study to validate its theoretical findings. According to the research, vaccination campaigns can help prevent HPV infection and reduce the risk of cervical cancer. Yunus and Olayiwola [18] highlighted the significance of COVID-19 vaccinations for Nigeria's pandemic control plan. It uses mathematical modeling at the fractional order to evaluate the duration, effectiveness, and impact of immunization campaigns. The findings indicate that immunization strategies with integer ordering are particularly effective in stopping the COVID-19 virus from spreading. As a critical public health measure, the study emphasizes the need for coordinated international efforts to increase vaccination uptake. According to Akogwu [19], the Differential Transform Method (DTM) was employed to obtain the series solution of the SIRV COVID-19 model in Nigeria. The validity of the DTM in solving the model was confirmed through comparison with Maple 21's Classical fourth-order Runge-Kutta method (RK4). The comparison between DTM and RK4 solutions showed a good correlation, validating the accuracy and efficiency of the DTM in solving the model.

The following are the goals of this paper:

- In the fractional instance, establish conditions that guarantee the existence and uniqueness of the model's solution.
- Describe the Lyapunov function approach's stability study of the endemic equilibrium point.
- perform the sensitivity analysis of the model
- Utilizing the fractional Adams–Bashforth–Moulton approach, ascertain numerical solutions.

We found that no research has evaluated the transmission dynamics and control of Diphtheria using a fractional calculus approach combined with the Adams–Bashforth–Moulton method to obtain numerical simulations of the model, despite reviewing several studies on mathematical models and transmission dynamics.

The rest of this essay is structured as follows: The model's formulation is covered in Section 2, its analysis is presented in Section 3, the fractional-order model's numerical findings are presented in Section 4, and concluding thoughts are provided in Section 5.

1.1 Preliminary

In this section, we cover several fundamental concepts and findings from fractional calculus. In this investigation, the fractional Caputo derivatives on the right and left will be utilized [20],[21] . The use of fractional calculus to simulate real-world issues in physics, engineering, biomathematics, and other scientific domains is also highlighted in this work.

Definition 1: let $f \in \Lambda^{\infty}(R)$, then the right and left Function's Caputo fractional derivative f is given by:

$$ {}^{b}D_{t}^{\alpha} f(t) = \left(t^{0}D_{t}^{-(p-\alpha)} \left(\frac{d}{dt} \right)^{p} f(t) \right) $$

$$ {}^{b}D_{t}^{\alpha} f(t) = \frac{1}{\Gamma(p-\alpha)} \int_{0}^{t} \left((t-\lambda)^{p-\alpha-1} f^{p}(\lambda) \right) d\lambda \tag{1} $$

similarly

$$ {}_{T}^{b}D_{t}^{\alpha}f(t)=\left({}_{t}D_{T}^{-(p-\alpha)}\left(\frac{-d}{dt}\right)^{p}f(t)\right) $$

$$ {}_{T}^{b}D_{T}^{\alpha}f(t)=\frac{(-1)^{p}}{\Gamma\left(p-\alpha\right)}\int_{t}^{T}\left((\lambda-t)^{p-\alpha-1}f^{p}\left(\lambda\right)\right)d\lambda $$

Definition 2: The Mittag-Leffler function in generalized form $E_{\phi,\beta}\left(x\right)$ for $x\in R$ is given by:

$$ E_{\phi,\beta}\left(x\right)=\sum_{p=0}^{\infty}\frac{x^{p}}{\Gamma\left(\phi p+\beta\right)},\ \alpha,\beta>0 \tag{2} $$

This alternatively can be shown as

$$ E_{\phi,\beta}\left(x\right)=xE_{\phi,\phi+\beta(x)}+\frac{1}{\Gamma\left(\beta\right)} \tag{3} $$

The function $t^{\beta-1}E_{\phi,\beta}\left(\pm\psi t^{\phi}\right)$is Laplace transformed as

$$ L\left[t^{\beta-1}E_{\phi,\beta(\pm\psi t^{\phi})}\right]\ =\frac{S^{\phi-\beta}}{S^{\phi}\pm\psi} \tag{4} $$

1.2 Proposition

Let $f\in\Lambda^{\infty}(R)\cap b\left(R\right)$ and $\phi\in R,\ p-1<\phi<p$, Consequently, the following requirements are met:

- $$ {}_{t_0}^{b}D_{t}^{\alpha}I^{\alpha}f\left(t\right)=f\left(t\right) $$
- $$ I_{t_0}^{\alpha}D_{t}^{\alpha}f\left(t\right)=f\left(t\right)-\sum\nolimits_{k=0}^{p-k}\frac{t^{k}}{k!}f^{k}\left(t_{o}\right). $$

2 Methodology/Model formulation

The total number of individuals at time t, indicated $N(t)$, is divided into (7) mutually exclusive compartments of susceptible individual $S_d(t)$, Exposed individuals to diphtheria$E_d\left(t\right)$, Vaccinated individual with diphtheria $V_d\left(t\right)$, infected individual with diphtheria $I_d\left(t\right)$, treatment class for individuals with diphtheria$T_d\left(t\right)$, Bacteria Class $B(t)$, and Set of individual that recovered from the disease $R_d\left(t\right)$. Humans' population is represented as;

$$ N\left(t\right)=S_d\left(t\right)+E_d\left(t\right)+I_d\left(t\right)+T_d\left(t\right)+V_d\left(t\right)+R_d\left(t\right) $$

The bacteria class is denoted $B(t)$

Diphtheria Susceptible Individuals S_d is recruited at the rate of Λ, the class reduces by natural death rate μ as well as by the percentage of those that contract the disease after coming into touch with a human who has diphtheria I_d at rates of β and β_1. This class also reduces by the rate α, These susceptible individuals grow by the rate ψ at which the vaccination wanes so that the vaccinated become susceptible again at the rate ω. the dynamics of this class is formulated as;

$$ \frac{dS_d}{dt}=\Lambda-\left(\frac{\beta IS}{N}+\frac{\beta_1 B}{K+B}\right)S_d+\omega R_d+\psi V_d-\alpha S_d-\mu S_d $$

Diphtheria Exposed Individuals E_d rises due to the percentage of people who contract new infections at a rate of β and β_1 respectively. This class reduces by the rate at which the exposed becomes fully infected at rate θ and by natural death rate μ. This population is formulated as follows;

$$\frac{dE_d}{dt} = \left(\frac{\beta I_d S_d}{N} + \frac{\beta_1 B}{K+B}\right) S_d - (\theta + \mu) E_d$$

Diphtheria infected Individuals I_d grows as a result of the exposed class's advancement to the infected class at rate θ. this class reduces by natural mortality rate μ , death due to disease at rate $\delta$and the rate at which the infected are taken for treatment σ, The dynamics of this class is formulated as;

$$\frac{dI_d}{dt} = \theta E_d - (\sigma + \delta + \mu) I_d$$

Diphtheria infected Individuals T_d increases in proportion to the rate at which the afflicted are treated σ, due to both disease induced and natural death at rate δ and μ respectively. Finally, the class reduces as a result of recovery at the rate ε of the treated individuals. The following is a presentation of this population's dynamics;

$$\frac{dT_d}{dt} = \sigma I_d - (\varepsilon + \phi\delta + \mu) T_d$$

Vaccinated individuals against diphtheria V_d population grows due to vaccination rate α and eventually diminishes as a result of the declining vaccination rate and natural death at rate ψ and μ respectively. The dynamics of people who have received a diphtheria vaccination are modeled as follows;

$$\frac{dV_d}{dt} = \alpha S_d - (\psi + \mu) V_d$$

Bacteria class B population grows due to the shedding rate of the bacteria into the infected and treatment classes at the rate P_1 and P_2 respectively. The population reduces by natural death rate μ_B. The following is a presentation of this population's dynamics;

$$\frac{dB}{dt} = P_1 I_d + P_2 T_d - \mu_B B$$

Diphtheria recovered individuals R_d grows due to treatment recovery rate ε. The class eventually decreases because of how quickly the recovered individuals become vulnerable at the rate ω and natural death rate μ.

$$\frac{dR_d}{dt} = \varepsilon T_d - (\omega + \mu) R_d$$

The population-related force of infection is $\lambda = \frac{\beta I_d S_d}{N} + \frac{\beta_1 B}{K+B}$

The model flow diagram that aligns with our hypothesis is displayed in Fig. 1; Similarly, the following describes the mathematical model that matches our presumptions and the above description:

$$\left.\begin{array}{l} \frac{dS_d}{dt} = \Lambda - \lambda S_d + \omega R_d + \psi V_d - \alpha S_d - \mu S_d, \\ \frac{dE_d}{dt} = \lambda S_d - (\theta + \mu) E_d, \\ \frac{dI_d}{dt} = \theta E_d - (\sigma + \delta + \mu) I_d, \\ \frac{dT_d}{dt} = \sigma I_d - (\varepsilon + \phi\delta + \mu) T_d, \\ \frac{dV_d}{dt} = \alpha S_d - (\psi + \mu) V_d, \\ \frac{dB}{dt} = P_1 I_d + P_2 T_d - \mu_B B, \\ \frac{dR_d}{dt} = \varepsilon T_d - (\omega + \mu) R_d. \end{array}\right\} \quad (5)$$

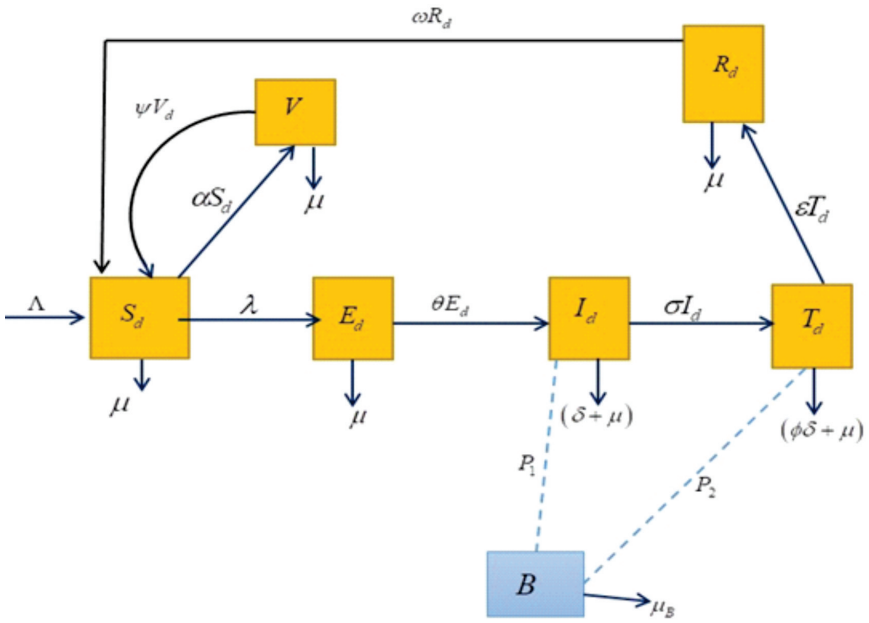

Figure 1: model schematic flow diagram.

2.1 Fractional Diphtheria mathematical model

Using the Caputo fractional derivative operator, we expand the integer model of Diphtheria given in Eq. (5) in this section. Compared to the classical model given in Eq. (5), the new model presented using the Caputo fractional derivative operator has a higher degree of freedom because the output of the fractional order model can be modified to have different responses. Thus, the fractional Diphtheria technique is explained as follows:

$$\left.\begin{aligned} {}^{b}D_t^{\alpha}S_d &= \Lambda - \lambda S_d + \omega R_d + \psi V_d - \alpha S_d - \mu S_d,\\ {}^{b}D_t^{\alpha}E_d &= \lambda S_d - M_1 E_d,\\ {}^{b}D_t^{\alpha}I_d &= \theta E_d - M_2 I_d,\\ {}^{b}D_t^{\alpha}T_d &= \sigma I_d - M_3 T_d,\\ {}^{b}D_t^{\alpha}V_d &= \alpha S_d - M_4 V_d,\\ {}^{b}D_t^{\alpha}B &= P_1 I_d + P_2 T_d - \mu_B,\\ {}^{b}D_t^{\alpha}R_d &= \varepsilon T_d - M_5 R_d. \end{aligned}\right\} \tag{6}$$

Where $M_1 = (\theta + \mu)$, $M_2 = (\sigma + \delta + \mu)$, $M_3 = (\varepsilon + \phi\delta + \mu)$, $M_4 = (\psi + \mu)$, and $M_5 = (\omega + \mu)$. Assuming favorable initial conditions

$$S_d(0) = S_{d0}, E_d(0) = E_{d0}, I_d(0) = I_{d0}, T_d(0) = T_{d0}, V_d(0) = V_{d0}, B(0) = B_0, R_d(0) = R_{d0}. \tag{7}$$

3 Analysis of the model

3.1 Positivity of model solution

We took the initial values' non-negativity into account.

$$\lim Sup.N(t) \leq \frac{\lambda}{\mu},$$

Secondly, If $\lim Sup.N_0(t) \leq \frac{\lambda}{\mu}$, then the feasible domain of our model is provided by;

$$\Omega = \left\{ (S_d, E_d, I_d, T_d, V_d, B, R_d) \subset R_+^7 : S_d + E_d + I_d + T_d + V_d + B + R_d \leq \frac{\lambda}{\mu}, \right\}$$

so that

$$\Omega \subset R_+^7,$$

Hence $\Omega$is positively invariant.

if $S_{d0}, E_{d0}, I_{d0}, T_{d0}, V_{d0}, B_0, R_{d0}$ are non-negative, therefore model (6)'s solution will also be non-negative for $t > 0$ Selecting the first equation from Eq. (6), we have that

$${}^bD_t^\alpha S_d = \Lambda - (\lambda + \alpha + \mu) S_d + \omega R_d + \psi V_d,$$

$${}^bD_t^\alpha S_d + (\lambda + \alpha + \mu) S_d = \Lambda + \omega R_d + \psi V_d,$$

But

$$\Lambda + \omega R_d + \psi V_d \geq 0,$$

then

$${}^bD_t^\alpha S_d + (\lambda + \alpha + \mu) S_d \geq 0$$

Using the acquired Laplace transform;

$$L\left[{}^bD_t^\alpha S_d\right] + L\left[(\lambda + \alpha + \mu) S_d\right] \geq 0$$

$$S^\alpha S_d(s) - S^{\alpha-1} S_d(0) + (\lambda + \alpha + \mu) S_d(s) \geq 0,$$

$$S_d(t) \geq \frac{S^{\alpha-1}}{(S^\alpha + (\lambda + \alpha + \mu))} S_{d0}.$$

Using the inverse Laplace transform, we were able to obtain;

$$S_d(t) \geq E_{\alpha,1}\left(-(\lambda + \alpha + \mu)\right) S_{d0} \tag{8}$$

Given that the term in Eq. (8) on the right is positive, we can now deduce that $S_d \geq 0$ for $t \geq 0$ In the same way, we also have that $E_d \geq 0\,, I_d \geq 0\,, T_d \geq 0\,, V_d \geq 0\,, B \geq 0\,, R_d \geq 0$, since they are positive aspects, the solution will continue to be in for all with positive initial conditions.

3.2 Boundedness of fractional model solution

The total number of people in our model is provided by;

$$N(t) = S_d(t) + E_d(t) + I_d(t) + T_d(t) + V_d(t) + R_d(t).$$

Thus, using our fractional model (6), we can now

$${}^bD_t^\alpha N(t) = {}^bD_t^\alpha S_d(t) + {}^bD_t^\alpha E_d(t) + {}^bD_t^\alpha I_d(t) + {}^bD_t^\alpha T_d(t) + {}^bD_t^\alpha V_d(t) + {}^bD_t^\alpha R_d(t).$$

$${}^bD_t^\alpha N(t) = \Lambda - \mu N(t) \tag{9}$$

Using (9)'s Laplace transformation, we arrived at;

$$L\left[{}^{b}D_{t}^{\alpha}N(t)\right] \leq L\left[\Lambda - \mu N\left(t\right)\right],$$

$$S^{\alpha}N(S) - S^{\alpha-1}N(0) + \mu N(S) \leq \frac{\lambda}{S},$$

$$N(s) \leq \frac{S^{\alpha-1}}{(S^{\alpha}+\mu)}N(0) + \frac{\Lambda}{S\left(S^{\alpha}+\mu\right)} \tag{10}$$

Taking Eq. (10)'s inverse Laplace transform gave us;

$$N(t) \leq E_{\alpha,1}\left(-\mu t^{\alpha}\right)N(0) + \Lambda E_{\alpha,\alpha+1}\left(-\mu t^{\alpha}\right) \tag{11}$$

At $t \to \infty$, the limit of Eq. (11) becomes

$$\lim_{t\to\infty} SupN\left(t\right) = \frac{\Lambda}{\mu}.$$

This means that, if $N \leq \frac{\Lambda}{\mu}$ which implies that, $N(t)$is bounded. We therefore draw the conclusion that epidemiologically, this region Ω is similarly plausible and well posed.

3.3 Existence and uniqueness of our model solution

Let T be a real nonnegative number, given that $Z = [0, T]$. The collection of every continuous function defined on$Z$ is denoted by $N_e^0 Z$ with norm as

$$\|G\| = \sup\left\{\left|G\left(t\right)\right| t, \in Z\right\}.$$

Taking into account model (6) with the starting conditions given in (7), which is modeled as an initial value problem (IVP) in (12)

$$D_t^{\alpha}G\left(t\right) = Q\left(t, G\left(x\right)\right), 0 < t < T < \infty,$$

$$G\left(0\right) = G_0. \tag{12}$$

where $G\left(t\right) = \left(S_d\left(t\right), E_d\left(t\right), I_d\left(t\right), T_d\left(t\right), V_d\left(t\right), B\left(t\right), R_d\left(t\right)\right)$ symbolizes the classes, and Q is a continuous function with the following definition;

$$Q_1\left(t, G\left(t\right)\right) = \begin{pmatrix} Q_1\left(t, S_d\left(t\right)\right) \\ Q_2\left(t, E_d\left(t\right)\right) \\ Q_3\left(t, I_d\left(t\right)\right) \\ Q_4\left(t, T_d\left(t\right)\right) \\ Q_5\left(t, V_d\left(t\right)\right) \\ Q_6\left(t, B\left(t\right)\right) \\ Q_7\left(t, R_d\left(t\right)\right) \end{pmatrix} = \begin{pmatrix} \Lambda - \left(\frac{\beta IS}{N} + \frac{\beta_1 B}{K+B}\right)S_d + \omega R_d + \psi V_d - \alpha S_d - \mu S_d \\ \left(\frac{\beta I_d S_d}{N} + \frac{\beta_1 B}{K+B}\right)S_d - \left(\theta + \mu\right)E_d \\ \theta E_d - \left(\sigma + \delta + \mu\right)I_d \\ \sigma I_d - \left(\varepsilon + \phi\delta + \mu\right)T_d \\ \alpha S_d - \left(\psi + \mu\right)V_d \\ P_1 I_d + P_2 T_d - \mu_B \\ \varepsilon T_d - \left(\omega + \mu\right)R_d \end{pmatrix} \tag{13}$$

Using proposition (2.1), we have that,

$$\begin{gathered}
S_d(t) = S_{d0} + I_t^{\alpha}\left[\Lambda - \left(\frac{\beta IS}{N} + \frac{\beta_1 B}{K+B}\right) S_d + \omega R_d + \psi V_d - \alpha S_d - \mu S_d\right], \\
E_d(t) = E_{d0} + I_t^{\alpha}\left[\left(\frac{\beta I_d S_d}{N} + \frac{\beta_1 B}{K+B}\right) S_d - (\theta+\mu) E_d\right] \\
I_d(t) = I_{d0} + I_t^{\alpha}\left[\theta E_d - (\sigma+\delta+\mu) I_d\right], \\
T_d(t) = T_{d0} + I_t^{\alpha}\left[\sigma I_d - (\varepsilon+\phi\delta+\mu) T_d\right], \\
V_d(t) = V_{d0} + I_t^{\alpha}\left[\alpha S_d - (\psi+\mu) V_d\right], \\
B(t) = B_0 + I_t^{\alpha}\left[P_1 I_d + P_2 T_d - \mu_B\right], \\
R_d(t) = R_d + I_t^{\alpha}\left[\varepsilon T_d - (\omega+\mu) R_d\right].
\end{gathered} \tag{14}$$

Here is how we get the Picard iteration of (14):

$$\begin{gathered}
S_d(t) = S_{d0} + \frac{1}{\Gamma(\alpha)}\int_0^t (t-\lambda)^{\alpha-1} Q_1\left(\lambda, S_{d(n-1)}(\lambda)\right) d\lambda, \\
E_d(t) = E_{d0} + \frac{1}{\Gamma(\alpha)}\int_0^t (t-\lambda)^{\alpha-1} Q_2\left(\lambda, E_{d(n-1)}(\lambda)\right) d\lambda, \\
I_d(t) = I_{d0} + \frac{1}{\Gamma(\alpha)}\int_0^t (t-\lambda)^{\alpha-1} Q_3\left(\lambda, I_{d(n-1)}(\lambda)\right) d\lambda, \\
T_d(t) = T_{d0} + \frac{1}{\Gamma(\alpha)}\int_0^t (t-\lambda)^{\alpha-1} Q_4\left(\lambda, T_{d(n-1)}(\lambda)\right) d\lambda, \\
V_d(t) = V_{d0} + \frac{1}{\Gamma(\alpha)}\int_0^t (t-\lambda)^{\alpha-1} Q_5\left(\lambda, V_{d(n-1)}(\lambda)\right) d\lambda, \\
B(t) = B_0 + \frac{1}{\Gamma(\alpha)}\int_0^t (t-\lambda)^{\alpha-1} Q_6\left(\lambda, B_{(n-1)}(\lambda)\right) d\lambda, \\
R_d = R_{d0} + \frac{1}{\Gamma(\alpha)}\int_0^t (t-\lambda)^{\alpha-1} Q_7\left(\lambda, R_{d(n-1)}(\lambda)\right) d\lambda.
\end{gathered} \tag{15}$$

Now, we changed the initial value problem in Eq. (12) to get ;

$$G(t) = G(0) + \frac{1}{\Gamma(\alpha)}\int_0^t (t-\lambda)^{\alpha-1} Q(\lambda, G(\lambda))\, d\lambda. \tag{16}$$

Lemma 1, Vector satisfies the Lipchitz requirement as stated in Eq. (13) $Q(t, G(t))$ on a set $[0,T]\times R_+^7$ with the Lipchitz constant given as;

$$\zeta = \max\left(\begin{array}{l}(\beta^* + \beta_1^* + \mu), (\theta+\mu), (\sigma+\delta+\mu), (\varepsilon+\phi\delta+\mu), \\ \mu_B, (\psi+\mu), (\omega+\mu).\end{array}\right)$$

Proof

$$\begin{gathered}
\|Q_1(t,S) - Q_1(t,S)\| \\
\left\| \begin{array}{l} \Lambda - \left(\left(\frac{\beta IS}{N} + \frac{\beta_1 B}{K+B}\right) + \mu\right) S_d - \alpha S_d + \omega R_d + \psi V_d \\ - \left(\Lambda - \left(\left(\frac{\beta IS}{N} + \frac{\beta_1 B}{K+B}\right) + \mu\right)\right) S_{d1} - (\alpha S_d + \omega R_d + \psi V_d) \end{array} \right\| \\
\left\| - \left(\frac{\beta IS}{N} + \frac{\beta_1 B}{K+B}\right)(S_d - S_{d1}) + \mu(S_d - S_{d1}) \right\|
\end{gathered}$$

$$\leq \left(\beta_1^* + \beta_{1,2}^*\right) \|(S_d - S_{d1})\| + \|\mu\,(S_d - S_{d1})\|$$

$$\|Q_1\,(t, S_d) - Q_1\,(t, S_{d1})\| \leq \left(\beta_1^* + \beta_{1,2}^* + \mu\right) \|S_d - S_{d1}\|\,.$$

Likewise, we discovered the following:

$$\begin{aligned}
\|Q_2\,(t, E_d) - Q_2\,(t, E_{d1})\| &\leq (\theta + \mu)\,\|E_d - E_{d1}\|\,, \\
\|Q_3\,(t, I_d) - Q_3\,(t, I_{d1})\| &\leq (\sigma + \delta + \mu)\,\|I_d - I_{d1}\|\,, \\
\|Q_4\,(t, T_d) - Q_4\,(t, T_{d1})\| &\leq (\varepsilon + \phi\delta + \mu)\,\|T_d - T_{d1}\|\,, \\
\|Q_5\,(t, V_d) - Q_5\,(t, V_{d1})\| &\leq (\psi + \mu)\,\|V_d - V_{d1}\|\,, \\
\|Q_6\,(t, B) - Q_6\,(t, B_1)\| &\leq \mu_B\,\|B - B_1\|\,, \\
\|Q_7\,(t, R_d) - Q_7\,(t, R_{d1})\| &\leq (\omega + \mu)\,\|R_d - R_{d1}\|\,,
\end{aligned} \tag{17}$$

Where we obtained

$$\|Q\,(t, G\,(t)) - Q\,(t, G_2\,(t))\| \leq \zeta\,\|G_1 - G_2\|\,.$$

$$\zeta = \max\left(\begin{array}{l} (\beta^* + \beta_1^* + \mu)\,, (\theta + \mu)\,, (\sigma + \delta + \mu)\,, (\varepsilon + \phi\delta + \mu)\,, \\ \mu_B, (\psi + \mu)\,, (\omega + \mu)\,. \end{array}\right) \tag{18}$$

Lemma 2. There is a solution to the initially value problems (6), (7) in Eq. (18).

$$G\,(t) \in L_c^0\,(F)\,.$$

We examine the solution of using fixed point theory and Picard-Lindel of $G\,(t) = S\,(G\,(t))$, When the Picard operator, represented as S, is defined as;

$$S : L_C^0\left(F, R_+^*\right) \to L_C^0\left(F, R_+^7\right).$$

$$S\,(G\,(t)) = G\,(0) + \frac{1}{\Gamma\,(\alpha)} \int_0^t (t - \lambda)^{\alpha - 1} G\,(\lambda, G\,(\lambda))\,d\lambda$$

$$\|S\,(G_1\,(t)) - S\,(G_2\,(t))\|$$

$$\left\| \frac{1}{\Gamma\,(\alpha)} \int_0^t (t - \lambda)^{\alpha - 1}\,[Q\,(\lambda, G_1\,(\lambda)) - Q\,(\lambda, G_2\,(\lambda))\,d\lambda] \right\|$$

$$\leq \frac{1}{\Gamma\,(\alpha)} \int_0^t (t - \lambda)^{\alpha - 1}\,\|Q\,(\lambda, G_1\,(\lambda)) - Q\,(\lambda, G_2\,(\lambda))\,d\lambda\|$$

$$\leq \frac{\zeta}{\Gamma\,(\alpha)} \int_0^t (t - \lambda)^{\alpha - 1}\,\|G_1 - G_2\|\,d\lambda$$

$$\|S\,(G_1\,(t)) - S\,(G_2\,(t))\| \leq \frac{\zeta}{\Gamma\,(\alpha + 1)\,S}$$

$\frac{\zeta}{\Gamma(\alpha+1)} S \leq 1$ the answer to Eqs. (6) and (7) is unique since the Picard operator produces a contradiction.

3.4 The basic reproduction number R_0 and model equilibrium points

The model (5)'s disease-free equilibrium point can be written as follows:

$$DDFEP = \left\{S_d^*, E_d^*, I_d^*, T_d^*, B^*, R_d^*\right\} = \left\{\frac{\Lambda\left(\alpha+\mu\right)}{\alpha\mu+\psi\mu+\mu^2}0,0,0,0,\frac{\Lambda\alpha}{\alpha\mu+\psi\mu+\mu^2},0\right\} \tag{19}$$

We utilize the procedure described by [22] to calculate the fundamental reproduction number.

Let $u = (E_d, I_d, T_d, B)$

So, that $\frac{du}{dt} = F - V$

Where; $F = \begin{bmatrix} 0 & \frac{\beta(\psi+\mu)}{\alpha+\psi+\mu} & 0 & \frac{\Lambda\beta_1}{\mu K} \\ 0 & 0 & 0 & 0 \\ 0 & 0 & 0 & 0 \\ 0 & 0 & 0 & 0 \end{bmatrix}$, $V = \begin{bmatrix} M_1 & 0 & 0 & 0 \\ -\theta & M_2 & 0 & 0 \\ 0 & -\sigma & M_3 & 0 \\ 0 & -P_1 & -P_2 & \mu_B \end{bmatrix}$ Mathematically, the basic reproduction number is computed as $R_0 = \rho\left(FV^{-1}\right)$ where ρ is the dominant Eigen value of the system is the dominant Eigen value of the system $\left(FV^{-1}\right)$. Where R_0^d is the basic reproduction number associated with the individuals in the population.

$$R_0 = \frac{\theta\left(\mu K M_3\mu_B\beta\left(\psi+\mu\right)+\left(\alpha+\psi+\mu\right)M_3P_1\Lambda\beta_1+\left(\alpha+\psi+\mu\right)P_2\sigma\Lambda\beta_1\right)}{\left(\alpha+\psi+\mu\right)M_1M_2\mu K M_3\mu_B} \tag{20}$$

Where $M_1 = (\theta+\mu)$, $M_2 = (\sigma+\delta+\mu)$, $M_3 = (\varepsilon+\phi\delta+\mu)$, $M_4 = (\psi+\mu)$, and $M_5 = (\omega+\mu)$.

3.5 Endemic equilibrium point

We looked into the potential for an endemic equilibrium point. Where the disease persists in the population, there is a positive stable state known as the endemic equilibrium point. The variables in the model are not zero at this equilibrium point.

$$(S_d^* \neq 0, E_d^* \neq 0,\ I_d^* \neq 0, T_d^* \neq 0, V_d^* \neq 0, B_d^* \neq 0 \; and \; R_H^* \neq 0)$$

The model equations are solved in terms of the force of infection linked with human populations in order to examine the endemic equilibrium point. Based on the fractional Diphtheria model (6), the endemic equilibrium state is symbolised as follows:

$$\eta^{**} = (S_d^{**}, E_d^{**},\ I_d^{**},\ T_d^{**}, V_d^{**}, B^{**},\ R_H^{**}),$$

Defined as;

$$S_d = \frac{\Lambda M_1M_2M_3M_4M_5}{M_2M_3M_5\left(\left(\alpha+\lambda+\mu\right)M_4-\alpha\psi\right)M_1-\lambda\omega\sigma\theta M_4}$$

$$E_d^{**} = \frac{\lambda\Lambda M_2M_3M_4M_5}{M_2M_3M_5\left(\left(\alpha+\lambda+\mu\right)M_4-\alpha\psi\right)M_1-\lambda\omega\sigma\theta M_4}$$

$$I_d^{**} = \frac{\theta\lambda\Lambda M_3M_4M_5}{M_2M_3M_5\left(\left(\alpha+\lambda+\mu\right)M_4-\alpha\psi\right)M_1-\lambda\omega\sigma\theta M_4}$$

$$T_d^{**} = \frac{\theta\lambda\Lambda M_4M_5\sigma}{M_2M_3M_5\left(\left(\alpha+\lambda+\mu\right)M_4-\alpha\psi\right)M_1-\lambda\omega\sigma\theta M_4}$$

$$V_d^{**} = \frac{\alpha\Lambda M_1M_2M_3M_5}{M_2M_3M_5\left(\left(\alpha+\lambda+\mu\right)M_4-\alpha\psi\right)M_1-\lambda\omega\sigma\theta M_4}$$

$$B^{**} = \frac{\left(\sigma P_2+M_3P_1\right)\Lambda M_5M_4\theta\lambda}{\mu_b\left(M_2M_3M_5\left(\left(\alpha+\lambda+\mu\right)M_4-\alpha\psi\right)M_1-\lambda\omega\sigma\theta M_4\right)}$$

$$R_d^{**} = \frac{\sigma M_4 \Lambda \theta \lambda}{M_2 M_3 M_5 \left(\left(\alpha + \lambda + \mu\right) M_4 - \alpha\psi\right) M_1 - \lambda\omega\sigma\theta M_4}$$

Where $M_1 = (\theta + \mu)$, $M_2 = (\sigma + \delta + \mu)$, $M_3 = (\varepsilon + \phi\delta + \mu)$, $M_4 = (\psi + \mu)$, and $M_5 = (\omega + \mu)$. Substituting the equations above into the force of infection $\lambda^{**} = \frac{\beta I}{N} + \frac{\beta_t B}{K+B}$ we obtained;

$$f(\lambda^{**}) = \lambda^{**} B_1 + B_2 = 0$$

$$B_1 = \left(\left(M_1 M_2 M_3 + \sigma\theta + M_2 M_3\right) M_5 + \sigma\theta\right) M_4 + \begin{pmatrix} -\sigma\theta P_2 - \theta M_3 P_1 + P_1\theta\left(\beta_1 + \beta\right) M_3 \\ +\sigma\theta P_2\left(\beta_1 + \beta\right) \end{pmatrix} M_5 {M_4}^2 \theta\omega\sigma$$
$$- \left(\left(M_1 M_2 M_3 + \sigma\theta + M_2 M_3\right) M_5 + \lambda\sigma\theta\right) M_4 - K M_1 M_2 M_3 \mu_b$$

$$B_2 = M_1 M_2 M_3 \left(\alpha + \lambda + \mu\right) M_5 \left(1 - \frac{\theta\left(\mu K M_3 \mu_B \beta\left(\psi + \mu\right) + \left(\alpha + \psi + \mu\right) M_3 P_1 \Lambda\beta_1 + \left(\alpha + \psi + \mu\right) P_2 \sigma\Lambda\beta_1\right)}{\left(\alpha + \psi + \mu\right) M_1 M_2 \mu K M_3 \mu_B}\right)$$

$$B_2 = M_1 M_2 M_3 \left(\alpha + \lambda + \mu\right) M_5 \left(1 - R_0\right)$$

From above we observed that for $\lambda^{**} > 1$ then $R_0 > 1$ Which implies that, the endemic equilibrium point of model (6) is stable.

3.6 Sensitivity Analysis of the Diphtheria Model

Sensitivity analysis is used to identify the factors that improve an infection's ability to spread and be controlled within a population. With regard to any parameter, let's say p, the sensitivity index of the reproduction number of the Diphtheria model is as follows:

$$\Im_p^{R_0} = \frac{\partial R_0}{\partial p} \times \frac{p}{R_0}$$

$$R_0 = \frac{\theta\left(\mu K M_3 \mu_B \beta\left(\psi + \mu\right) + \left(\alpha + \psi + \mu\right) M_3 P_1 \Lambda\beta_1 + \left(\alpha + \psi + \mu\right) P_2 \sigma\Lambda\beta_1\right)}{\left(\alpha + \psi + \mu\right) M_1 M_2 \mu K M_3 \mu_B}$$

$$\Im_\beta^{R_0} = \frac{\mu K \mu_B \left(\psi + \mu\right)\left(\delta\phi + +\mu\right)\beta}{\left(\alpha + \psi + \mu\right)\left(P_1\mu + \left(\delta\phi +\right) P_1 + \sigma P_2\right)\Lambda\beta_1 + \mu K \mu_B \left(\psi + \mu\right)\left(\delta\phi + +\mu\right)\beta} = 0.1003$$

$$\Im_\theta^{R_0} = \frac{\mu}{\theta + \mu} = 0.0763$$

$$\Im_\phi^{R_0} = -\frac{\delta\left(\alpha + \psi + \mu\right) P_2 \sigma\Lambda\beta_1\phi}{\left(\delta\phi + +\mu\right)\left(\left(\alpha + \psi + \mu\right)\left(P_1\mu + \left(\delta\phi +\right) P_1 + \sigma P_2\right)\Lambda\beta_1 + \mu K \mu_B \left(\psi + \mu\right)\left(\delta\phi + +\mu\right)\beta\right)} = -0.0008$$

$$\Im_\psi^{R_0} = \frac{\mu K \mu_B \alpha\beta\left(\delta\phi + +\mu\right)\psi}{\left(\alpha + \psi + \mu\right)\left(\left(\alpha + \psi + \mu\right)\left(P_1\mu + \left(\delta\phi +\right) P_1 + \sigma P_2\right)\Lambda\beta_1 + \mu K \mu_B \left(\psi + \mu\right)\left(\delta\phi + +\mu\right)\beta\right)} = 0.0516$$

$$\Im_\alpha^{R_0} = -\frac{\mu K \mu_B \left(\psi + \mu\right)\left(\delta\phi + +\mu\right)\beta\alpha}{\left(\alpha + \psi + \mu\right)\left(\left(\alpha + \psi + \mu\right)\left(P_1\mu + \left(\delta\phi +\right) P_1 + \sigma P_2\right)\Lambda\beta_1 + \mu K \mu_B \left(\psi + \mu\right)\left(\delta\phi + +\mu\right)\beta\right)} = -0.0532$$

$$\Im_\delta^{R_0} = -0.0159$$

$$\Im_\varepsilon^{R_0} = -\frac{\left(\alpha + \psi + \mu\right) P_2 \sigma\Lambda\beta_1}{\left(\delta\phi + +\mu\right)\left(\left(\alpha + \psi + \mu\right)\left(P_1\mu + \left(\delta\phi +\right) P_1 + \sigma P_2\right)\Lambda\beta_1 + \mu K \mu_B \left(\psi + \mu\right)\left(\delta\phi + +\mu\right)\beta\right)} = -0.4162$$

$$\Im_{P_1}^{R_0} = \frac{\left(\delta\phi + +\mu\right)\left(\alpha + \psi + \mu\right) P_1 \Lambda\beta_1}{\left(\alpha + \psi + \mu\right)\left(P_1\mu + \left(\delta\phi +\right) P_1 + \sigma P_2\right)\Lambda\beta_1 + \mu K \mu_B \left(\psi + \mu\right)\left(\delta\phi + +\mu\right)\beta} = 0.4615$$

$$\Im_\mu^{R_0} = -0.1441$$

$$\Im_{P_2}^{R_0} = \frac{\sigma\Lambda\beta_1 P_2\left(\alpha + \psi + \mu\right)}{\mu K \mu_B \left(\psi + \mu\right)\left(\delta\phi + +\mu\right)\beta + \left(\delta\phi + +\mu\right)\left(\alpha + \psi + \mu\right) P_1 \Lambda\beta_1 + \sigma\Lambda\beta_1 P_2\left(\alpha + \psi + \mu\right)} = 0.4383$$

$$\Im_{\mu_B}^{R_0} = -\frac{(\alpha+\psi+\mu)\,\Lambda\beta_1\,((\delta\phi++\mu)\,P_1+\sigma P_2)}{(\alpha+\psi+\mu)\,\Lambda\beta_1\,((\delta\phi++\mu)\,P_1+\sigma P_2)+\mu K\mu_B\,(\psi+\mu)\,(\delta\phi++\mu)\,\beta} = -0.8997$$

$$\Im_{\sigma}^{R_0} = -\frac{(\alpha+\psi+\mu)\,\Lambda\beta_1\,((\delta\phi++\mu)\,P_1+\sigma P_2)}{(\alpha+\psi+\mu)\,\Lambda\beta_1\,((\delta\phi++\mu)\,P_1+\sigma P_2)+\mu K\mu_B\,(\psi+\mu)\,(\delta\phi++\mu)\,\beta} = -0.4984$$

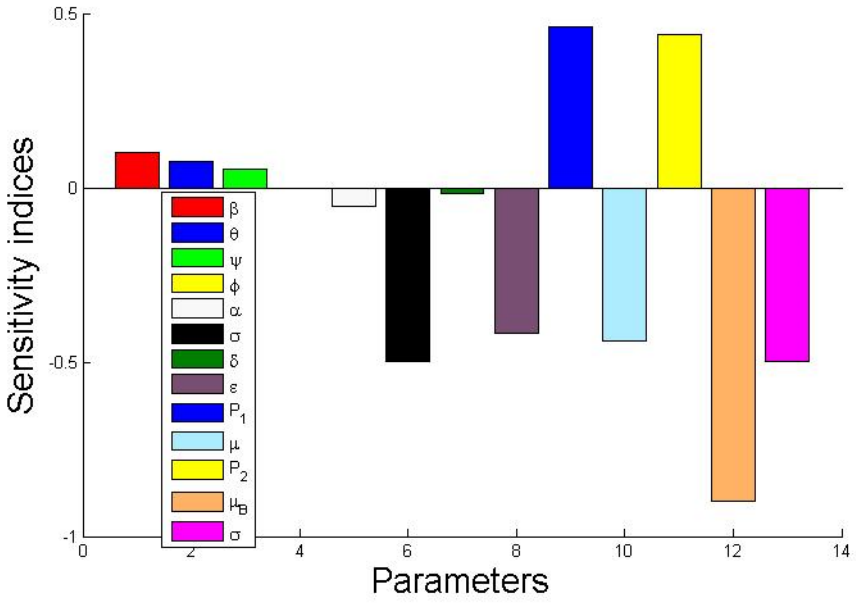

Figure 2: Bar chat of Diphtheria sensitivity Indices

3.7 Interpretation of the diphtheria Sensitivity Analysis

From the sensitivity analysis above, it is observed that the parameters like β, which is the contact rate of susceptible and infected humans, progression rate from exposed class to infected class θ, waning rate of vaccine ψ, shedding rate of bacteria P_1 and P_2 are all with positive sensitivity indices which enhances the spread of Diphtheria within the human population. Also the parameters like ϕ modification parameter that accounts for diphtheria induced death, rate at which susceptible individuals are vaccinated α, rate of treatment σ, the rate at which individuals under treatment recovered ε, disease induced death rate δ, Natural death rate μ and bacteria Natural death rate μ_B are with negative sensitivity indices and will reduces the prevalence of diphtheria within the humans population.

3.8 Global stability analysis at endemic equilibrium state

Using the direct Lyapunov approach for equilibrium point, the global stability is examined. When $R_0 > 1$, the endemic equilibrium point is globally stable, According to epidemiology, this implies that the disease will spread throughout the population regardless of the original population under consideration According to the fractional model (6).

$$\lambda = \frac{\beta I_d S_d}{N} + \frac{\beta_1 B}{K+B}$$

where

$$N \leq \frac{\lambda}{\mu}\ as\ t \to \infty$$

$$\lambda = \beta I_d S_d\,(K+B) + \mu(\beta_1 B)$$

Then, Our fractional model now becomes:

$$\left.\begin{array}{c} {}^{b}D_t^{\alpha}S_d = \Lambda - \lambda_1 S_d + \omega R_d + \psi V_d - \alpha S_d - \mu S_d \\ {}^{b}D_t^{\alpha}E_d = \lambda_1 S_d - M_1 E_d \\ {}^{b}D_t^{\alpha}I_d = \theta E_d - M_2 I_d \\ {}^{b}D_t^{\alpha}T_d = \sigma I_d - M_3 T_d \\ {}^{b}D_t^{\alpha}V_d = \alpha S_d - M_4 V_d \\ {}^{b}D_t^{\alpha}B = P_1 I_d + P_2 T_d - \mu_B \\ {}^{b}D_t^{\alpha}R_d = \varepsilon T_d - M_5 R_d \end{array}\right\} \tag{21}$$

The following outcomes of Equation (21) at equilibrium point
$\lambda = \Lambda - \lambda_1^{**} S_d^{**} + \omega R_d^{**} + \psi V_d^{**} - \alpha S_d^{**} - \mu S_d^{**} = \lambda_1^{**} S_d^{**} - M_1 E_d^{**} = \theta E_d^{**} - M_2 I_d^{**} = \sigma I_d^{**} - M_3 T_d^{**}$
$= \alpha S_d^{**} - M_4 V_d^{*8} = P_1 I_d^{**} + P_2 T_d^{**} - \mu_B B^{**} = \varepsilon T_d^{**} - M_5 R_d^{**}$

Theorem 1.
Model (21) is globally asymptotically stable if $R_0 > 1$
Whenever

$$\left(7 - \frac{S_d^*}{S} + \frac{\lambda_1}{\lambda_1^*}\left(1 - \frac{S_d E_d^*}{S_d^* E_d}\right) - \frac{I_d^* E_d}{I_d E_d^*} - \frac{T_d}{T_d^*} - \frac{T_d^* I_d}{T_d I_d^*}\right) \leq 0$$

Let

$$L(t) = L_H(t)$$

be the non-linear Lyaponov function shown in the following equation (22):

$$\begin{array}{l} L(t) = L_1\left(S_d - S_d^* - S_d^* In\frac{S_d}{S_d^*}\right) + L_2\left(E_d - E_d^* - E_d^* In\frac{E_d}{E_d^*}\right) + L_3\left(I_d - I_d^* - I_d^* In\frac{I_d}{I_d^*}\right) + \\ L_4\left(T_d - T_d^* - T_d^* In\frac{T_d}{T_d^*}\right) + L_5\left(V_d - V_d^* - V_d^* In\frac{V_d}{V_d^*}\right) + L_6\left(B_d - B_d^* - B_d^* In\frac{B_d}{B_d^*}\right) + \\ L_7\left(R_d - R_d^* - R_d^* In\frac{R_d}{R_d^*}\right) \end{array} \tag{22}$$

Using Eq. (22), we obtain the Caputo Fractional order derivative.

$$\begin{array}{l} {}^{b}D_t^{\alpha}L(t) = {}^{b}D_t^{\alpha}L_d(t) \leq L_1\left(1 - \frac{S_d^{**}}{S_d}\right){}^{b}D_t^{\alpha}S_d(t) + L_2\left(1 - \frac{E_d^{**}}{E_d}\right){}^{b}D_t^{\alpha}E_d(t) + L_3\left(1 - \frac{I_d^{**}}{I_d}\right)D_t^{\alpha}I_d(t) \\ +L_4\left(1 - \frac{T_d^{**}}{T_d}\right)D_t^{\alpha}T_d(t) + L_5\left(1 - \frac{V_d^{**}}{V_d}\right)D_t^{\alpha}V_d(t) + L_6\left(1 - \frac{B^{**}}{B}\right)D_t^{\alpha}B(t) \\ +L_7\left(1 - \frac{R_d^{**}}{R_d}\right)D_t^{\alpha}R_d(t) \end{array}$$

$$\begin{array}{l} = \lambda_d S_d^*\left(\left(1 - \frac{S_d^{**}}{S_d}\right){}^{b}D_t^{\alpha}S_d(t) + \left(1 - \frac{E_d^{**}}{E_d}\right){}^{b}D_t^{\alpha}E_d(t)\right) + L_3\left(1 - \frac{I_d^{**}}{I_d}\right){}^{b}D_t^{\alpha}I_d(t) + \left(1 - \frac{T_d^{**}}{T_d}\right){}^{b}D_t^{\alpha}T_d(t) \\ + \left(1 - \frac{V_d^{**}}{V_d}\right){}^{b}D_t^{\alpha}V_d(t) + \left(1 - \frac{B^{**}}{B}\right){}^{b}D_t^{\alpha}B_d(t) + \left(1 - \frac{R_d^{**}}{R_d}\right){}^{b}D_t^{\alpha}R_d(t) \end{array}$$

$$\left(1 - \frac{S_d^*}{S_d}\right){}^{b}D_t^{\alpha} = \left(1 - \frac{S_d^*}{S_d}\right)(\lambda_d^* S_d + \mu S_d^* + \omega R_d^* + \psi V_d^* + \alpha S_d^* - \lambda^* S_d - \omega R_d - \psi V_d + \alpha S_d - \mu S_d)$$

$$
\begin{aligned}
&= \lambda_d^* S_d^* \left(1 - \frac{S_d \lambda_{d1}}{S^{**}\lambda_{d1}^{**}} - \frac{S_d^*}{S_d} + \frac{\lambda_{d1}}{\lambda_{d1}^{**}}\right) + \mu S_d^* \left(2 - \frac{S_d}{S_d^*} - \frac{S_d^*}{S_d}\right) - \omega\left(1 - \frac{R_d}{R_d^*}\right) - \psi\left(1 - \frac{V_d}{V_d^*}\right)\left(1 - \frac{S_d^*}{S_d}\right), \\
\left(1 - \frac{E_d^{**}}{E_d}\right) {}^{b}D_t^{\alpha} E_d &= \left(1 - \frac{E_d^{**}}{E_d}\right)\left(\lambda_{d1}^{**} S_d - \lambda_{d1}^{**} S_d^{**} \frac{E_d}{E_d^{**}}\right), \\
&= \lambda_{d1}^{**} S^{**}\left(1 - \frac{S_d \lambda_{d1}}{S^{**}\lambda_{d1}^{**}} \frac{E_d^{**}}{E_d} - \frac{E_d^{**}}{E_d} + \frac{S_d \lambda_{d1}^{**}}{S^{**}\lambda_{d1}^{**}}\right), \\
\frac{M_1}{\theta}\left(1 - \frac{I_d^*}{I_d}\right) {}^{d}D_t^{\alpha} I_d &= \frac{M_2}{\theta}\left(1 - \frac{I_d^*}{I_d}\right)\left(\theta E_d - M_2 \frac{I_d}{I_d^{**}} I_d^*\right), \\
&= \lambda_{d1}^* S_d^*\left(1 + \frac{E_d}{E_d^*} - \frac{I_d}{I_d^*} - \frac{E_d I_d}{E_d^* I_d^*}\right), \\
\frac{M_1 M_2}{\sigma\theta}\left(1 - \frac{T_d^*}{T_a}\right) {}^{b}D_t^{\alpha} T_d &= \frac{M_1 M_2}{\sigma\theta}\left(1 - \frac{T_d^*}{T_a}\right)\left(\frac{I_d}{I_d^*} - \frac{T_d^*}{T_a}\right), \\
&= \lambda_{d1}^*\left(1 - \frac{T_a}{T_d^*} - \frac{I_d T_d^*}{I_d^* T_a} + \frac{I_d}{I_d^*}\right), \\
\frac{\alpha+\mu}{\alpha}\left(1 - \frac{V_d^*}{V_a}\right) {}^{b}D_t^{\alpha} V_d &= \frac{\alpha+\mu}{\alpha}\left(1 - \frac{V_d^*}{V_a}\right)\left(\alpha S_d - M_4 V_d^* \frac{V_d^*}{V_a}\right), \\
&= \lambda_{d1}^*\left(1 - \frac{S_a}{S_d^*} - \frac{V_d}{V_d^*} - \frac{V_d S_d^*}{V_d^* S_a}\right),
\end{aligned}
\tag{23}
$$

Hence, Eq. (23) now becomes;

$$
\begin{aligned}
&{}^{b}D_t^{\alpha} L(t) \leq \lambda_{d1}^{**} S_d^{**} \\
&\left(7 - \tfrac{S_d}{S_d^*} + \tfrac{\lambda_d}{\lambda_{d1}^*}\left(1 - \tfrac{S_d E_d^*}{S_d^* E_a}\right) - \tfrac{I_d E_d}{I_d^* E_d^*} - \tfrac{T_a}{T_d^*} - \tfrac{T_d I_d}{T_d^* I_d^*}\right) \\
&- (\alpha+\mu) S_d^* \lambda_{d1}^* \left(\left(\tfrac{S_d^*}{S_d} - 1 - In\tfrac{S_d^*}{S_d}\right) + \left(\tfrac{V_d^*}{V_d} - 1 - In\tfrac{V_d^*}{V_d}\right) + \left(\tfrac{R_d^*}{R_d} - 1 - In\tfrac{R_d^*}{R_d}\right)\right) \\
&- \psi V_d^* \lambda_{d1}^* S_d^* \left(1 - \tfrac{V_d}{V_d^*}\right)\left(1 - \tfrac{R_d}{R_d^*}\right)\left(1 - \tfrac{S_d}{S_d^*}\right)
\end{aligned}
$$

Which implies that, ${}^{b}D_t^{\alpha} L(t) \leq \lambda_{d1}^{**} S_d^{**} \beta \frac{(R_0 - 1)}{\mu} \Lambda S^{**}$

$$
\frac{-\beta(R_0-1)}{\mu}\Lambda S^{**}\left[\begin{array}{l}(\alpha+\mu) S_d^*\left(\left(\frac{S_d^*}{S_d} - 1 - In\frac{S_d^*}{S_d}\right) + \left(\frac{V_d^*}{V_d} - 1 - In\frac{V_d^*}{V_d}\right) + \left(\frac{R_d^*}{R_d} - 1 - In\frac{R_d^*}{R_d}\right)\right) \\ +\psi V_d^*\left(1 - \frac{V_d}{V_d^*}\right)\left(1 - \frac{R_d}{R_d^*}\right)\left(1 - \frac{S_d^*}{S_d}\right)\end{array}\right]
$$

Therefore, ${}^{b}D_t^{\alpha} L(t) \leq 0 \ for \ R_0 > 1$. This implies that $\eta^{**} = (S_d^{**}, E_d^{**}, I_d^{**}, I_d^{**}, T_d^{**}, R_d^{**})$, is the endemic equilibrium point, then it is globally asymptotically stable in Ω whenever $R_0 > 1$. according to LaSalle's invariance principle.

4 Fractional order model numerical results

We employed a numerical approach to solve the fractional order Diphtheria model, utilizing the generalized fractional Adams Bashforth–Moulton method described by [23] . Table 1 displays the values of the model parameters that were utilized, and also considers and simulates several values of the fractional order α.

4.1 Implementation of fractional Adams-Bashforth-Moulton method

In this work, the approach outlined by Baskonus and Bulut; Diethelm, is utilized [24],[25]. Using the fractional Adam–Bashforth–Moulton approach, we were able to derive an approximate solution of the

fractional Diphtheria model given in (6). The representation of the fractional model (6) in (23) is as follows:

$$ {}^{b}D_{t}^{\alpha}Y\left(t\right)=Z\left(t,Y\left(t\right)\right),\ 0<t<\varsigma, $$

$$ Y^{(n)}\left(0\right)=Y_{0}^{(n)},\ \ n=1,0,\ ...,Y,Y=[\alpha] \tag{24} $$

where $Y=\left(S_{d}^{*},E_{d}^{*},I_{d}^{*},T_{H}^{*},V_{d}^{*},B_{d}^{*},R_{H}^{*}\right)\in R_{+}^{7}$ and $P\left(t,Y\left(t\right)\right)$ is a real valued function that is continous.
Therefore, the following representation of Eq. (24) can be made using the idea of a fractional integral:

$$ Y\left(t\right)=\sum_{n=0}^{Y-1}Y_{0}^{(n)}\frac{t^{n}}{n!}+\frac{1}{\Gamma\left(\alpha\right)}\int_{0}^{t}\left(t-x\right)^{\alpha-1}P\left(x,Y\left(x\right)\right)dx \tag{25} $$

Using the method described by [24], we let the step size $h=\frac{\varsigma}{N},\ N\in\mathrm{N}$ with a grid that is uniform on $[0,\varsigma]$. Where $t_{c}=cr,\ c=0,1,1,\ ...N$ Therefore, the fractional order model of Diphtheria model presented in (6) can be approximated as:

$$ \begin{aligned}
S_{dk+1}\left(t\right)&=S_{d0}+\tfrac{h^{\gamma}}{\Gamma(\alpha+2)}\left\{\Lambda-\left(\beta I_{d}^{n}+\beta_{1}B^{n}\right)\tfrac{1}{N^{n}(K+B^{n})}+\omega R_{d}^{n}+\psi V_{d}^{n}-\alpha S_{d}^{n}-\mu S_{d}^{n}\right\}+\\
&\tfrac{h^{\alpha}}{\Gamma(\alpha+2)}\sum_{x=0}^{k}dx,k+1\left\{\lambda-\left(\beta I_{dx}+\beta_{1}B_{x}\right)\tfrac{1}{N_{x}}+\omega R_{dx}+\psi V_{dx}-\alpha S_{dx}-\mu S_{dx}\right\},\\
E_{dk+1}\left(t\right)&=E_{d0}+\tfrac{h^{\gamma}}{\Gamma(\alpha+2)}\left\{\left(\beta I_{d}^{n}+\beta_{1}B^{n}\right)\tfrac{S_{d}^{n}}{N^{n}(K+B)}-M_{1}E_{d}^{n}\right\}+\\
&\tfrac{h^{\alpha}}{\Gamma(\alpha+2)}\sum_{x=0}^{k}dx,k+1\left\{\left(\beta I_{dx}+\beta_{1}B_{x}\right)\tfrac{S_{dx}}{N_{x}(K+B_{x})}-M_{1}E_{dx}\right\},\\
I_{dk+1}\left(t\right)&=I_{d0}+\tfrac{h^{\gamma}}{\Gamma(\alpha+2)}\left\{\theta E_{d}^{n}-M_{2}I_{d}^{n}\right\}+\\
&\tfrac{h^{\alpha}}{\Gamma(\alpha+2)}\sum_{x=0}^{k}dx,k+1\left\{\theta E_{dx}-M_{2}I_{dx}\right\},\\
T_{dk+1}\left(t\right)&=T_{d0}+\tfrac{h^{\gamma}}{\Gamma(\alpha+2)}\left\{\sigma I_{d}^{n}-M_{3}T_{d}^{n}\right\}+\\
&\tfrac{h^{\alpha}}{\Gamma(\alpha+2)}\sum_{x=0}^{k}dx,k+1\left\{\sigma I_{dx}-M_{3}T_{dx}\right\},\\
T_{dk+1}\left(t\right)&=T_{d0}+\tfrac{h^{\gamma}}{\Gamma(\alpha+2)}\left\{\alpha S_{d}^{n}-M_{4}V_{d}^{n}\right\}+\\
&\tfrac{h^{\alpha}}{\Gamma(\alpha+2)}\sum_{x=0}^{k}dx,k+1\left\{\alpha S_{dx}-M_{4}V_{dx}\right\},\\
V_{dk+1}\left(t\right)&=V_{d0}+\tfrac{h^{\gamma}}{\Gamma(\alpha+2)}\left\{P_{1}I_{d}^{n}+P_{2}T_{d}^{n}-\mu_{B}B^{n}\right\}+\\
&\tfrac{h^{\alpha}}{\Gamma(\alpha+2)}\sum_{x=0}^{k}dx,k+1\left\{P_{1}I_{dx}+P_{2}T_{dx}-\mu_{B}B_{x}\right\},\\
R_{dk+1}\left(t\right)&=R_{d0}+\tfrac{h^{\gamma}}{\Gamma(\alpha+2)}\left\{\varepsilon T_{d}^{n}-M_{5}R_{d}^{n}\right\}+\\
&\tfrac{h^{\alpha}}{\Gamma(\alpha+2)}\sum_{x=0}^{k}dx,k+1\left\{\varepsilon T_{dx}-M_{5}R_{dx}\right\}.
\end{aligned} \tag{26} $$

Where

$$
\begin{aligned}
S_{dk+1}(t) &= \frac{1}{\Gamma(\alpha)}\sum_{x=0}^{k} e_x k+1\left\{\Lambda-(\beta I_{dx}+\beta_1 B_x)\frac{1}{N_x(K+B_x)}+\omega R_{dx}+\psi V_{dx}-\alpha S_{dx}-\mu S_{dx}\right\},\\
E_{dk+1}(t) &= \frac{1}{\Gamma(\alpha)}\sum_{x=0}^{k} e_x, k+1\left\{(\beta I_{dx}+\beta_1 B_x)\frac{S_{dx}}{N_x(K+B_x)}-M_1 E_{dx}\right\},\\
I_{dk+1}(t) &= \frac{1}{\Gamma(\alpha)}\sum_{x=0}^{k} e_x, k+1\{\theta E_{dx}-M_2 I_{dx}\},\\
T_{dk+1}(t) &= \frac{1}{\Gamma(\alpha)}\sum_{x=0}^{k} e_1, k+1\{\sigma I_{dx}-M_3 T_{dx}\},\\
T_{dk+1}(t) &= \frac{1}{\Gamma(\alpha)}\sum_{x=0}^{k} e_x, k+1\{\alpha S_{dx}-M_4 V_{dx}\},\\
V_{dk+1}(t) &= \frac{1}{\Gamma(\alpha)}\sum_{x=0}^{k} e_x, k+1\{P_1 I_{dx}+P_2 T_{dx}-\mu_B B_x\},\\
R_{dk+1}(t) &= \frac{1}{\Gamma(\alpha)}\sum_{x=0}^{k} e_1, k+1\{\varepsilon T_{dx}-M_5 R_{dx}\}.
\end{aligned}
\tag{27}
$$

Equations (25) and (26) provided us with;

$$dx,_{K+1} = K^{\alpha+1}-(k-\alpha)(k+\alpha)^{\alpha},\ x=0$$

$$(k-x+2)^{\alpha+1}+(k-\alpha)^{\alpha+1}-2(k-x+1)^{\alpha+1},\ 1\le x\le k$$

$$1, x=k+14$$

And

$$e_{x,k+1} = \frac{h^{\alpha}}{\alpha}\left[(k-x+1)^{\alpha}(k-x)^{\alpha}\right],\ 0\le x\le k$$

4.2 parameters descriptions

Table 1: Values of parameters used in the simulation.

Parameters	Symbol	Value (per day)	Source
Recruitment rate of individuals into the susceptible class	Λ	0.29	Assumed
Rate at which susceptible individuals come into contact with diphtheria	β	0.570	[26]
Rate at which exposed individuals progress to infection	θ	0.230	[27]
Rate at which individuals contact bacteria	β_1	0.341	Assumed
Rate at which infected individuals receive treatment	σ	0.36	Assumed
Recovery rate of treated individuals	ε	0.8	Assumed
Vaccination rate for susceptible individuals	α	0.500	[26]
Rate at which vaccine-induced immunity wanes	ψ	0.43	Assumed
Rate at which bacteria are shed into the environment	P_1, P_2	0.007	Assumed
Natural death rate of the bacteria	μ_B	0.047	Assumed
Natural death rate of humans	μ	0.019	[28]
Rate at which recovered individuals become susceptible again	ω	0.7	Assumed
Density of bacteria in the environment	K	0.005	Assumed
Death rate due to diphtheria	δ	0.006	[28]
Modification parameter for death in treated individuals	ϕ	0.1	Assumed

4.3 The fractional Adam-Bashforth Moulton approach is crucial for obtaining the model's numerical solutions

- The fractional Adam–Bashforth Moulton method attains high-order accuracy with just one extra function evaluation every step.
- This method is a helpful tool for numerical solutions of partial and fractional order differential equations and has potential applications in many fields, including engineering, chemistry, and medicine.
- The Adam–Bashforth Moulton method, which is frequently included in packaged ODE solvers, provides automatic error management.

4.4 Fractional order Diphtheria model simulation

In this section, we present the graphs obtained from numerical simulation of the fractional order Diphtheria.

A closer look at the surface plot in Fig. 3(a) indicates that a rise in the parameters and representing the contact rate between bacteria and susceptible humans, respectively, which increases the incidence of diphtheria in human populations, as demonstrated by the basic reproduction number surpassing one (1). The surface plot in Fig. 3(b) shows the effects of different between and , indicating the percentage of affected people receiving therapy and rate of vaccination in relation to the population's basic reproduction number . It was observed that an increase in these parameters leads to a peak in the value of to a numerical value below one. This implies that the burden of diphtheria among humans will eventually be reduced by improving the treatment rate of affected persons and putting policies in place to encourage vaccination rates. Figure 4(a) shows the impact of varying (the waning rate of the vaccine) and (the progression rate from exposed to infected) on the basic reproduction number . If appropriate measures are not implemented, these factors and can worsen the prevalence of diphtheria, as evidenced by their effect on the basic reproduction number, causing it to rise above one (1). The graph in Figure 4(b) presents a contour plot of in relation to . Analyzing

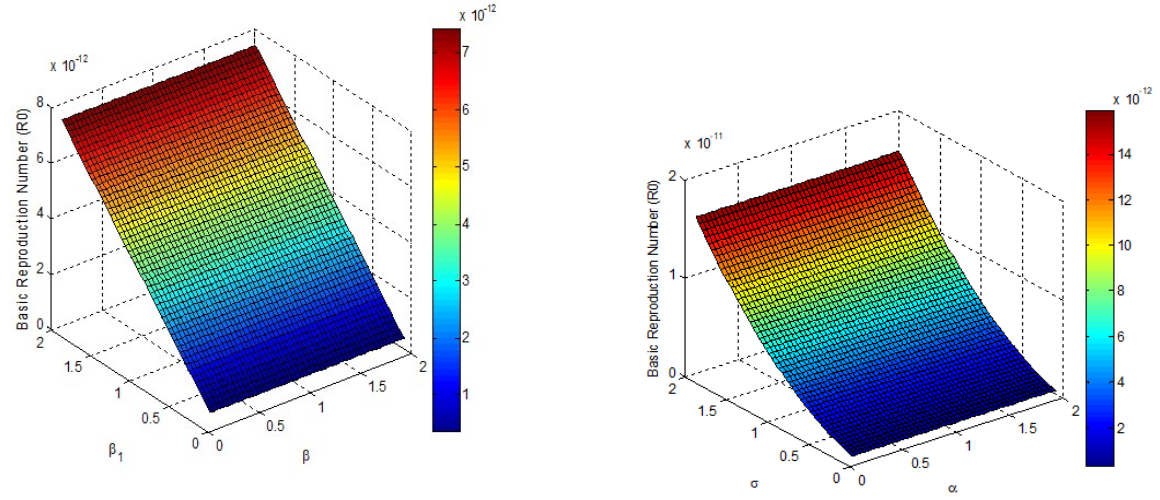

(a) **Impact of β and β_1 on R_0^d** (b) **Impact of σ and $alpha$ on R_0^d**

Figure 3: **surface plot of the basic reproduction number**

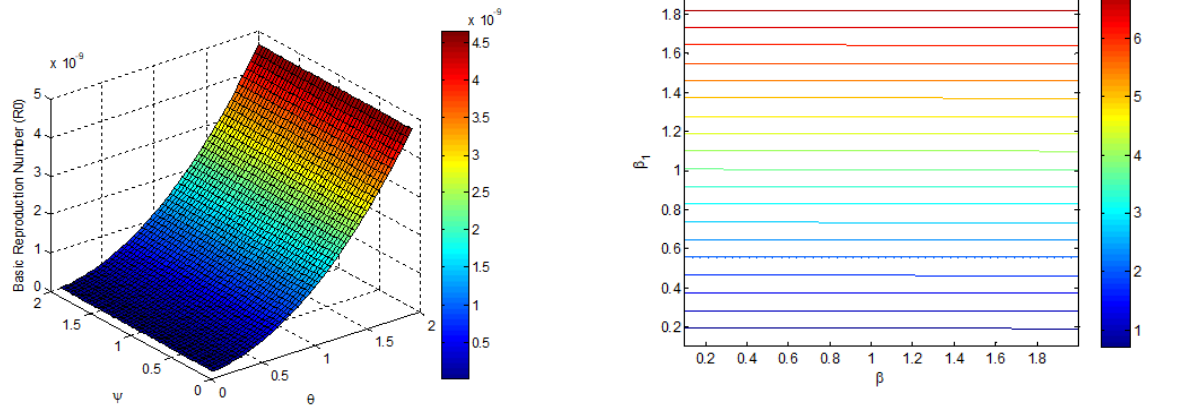

(a) **Impact of ψ and θ on R_0^d**

(b) **contour plot showing the Impact of β_1 and β on R_0^d**

Figure 4: **surface plot and contour plot of the basic reproduction number**

the numerical trends in the graph reveals that the maximum value reached by adjusting these parameters is 0.6, which is below unity (1). This observation indicates that increasing these parameters would not lead to a significant diphtheria outbreak in the population. Additionally, raising the values of (the treatment rate of infected individuals) and (the vaccination rate of susceptible individuals) would help reduce the burden of diphtheria among the population. This conclusion is supported by Figure 5(a), where stays below unity (1). The plot in Figure 5(b) shows the effect of varying the fractional order derivative on the susceptible human population over time. The plot clearly indicates that an increase in leads to a decline in the susceptible population. This reduction is due to the implementation of treatment and vaccination strategies, which lowers the number of individuals vulnerable to the disease. Figure 6(a) shows that the exposed population initially rises and then quickly declines as infection rates increase. This indicates that despite the overall population decreasing due to higher infectiousness, there is still a flow of individuals from the susceptible class into the exposed class.

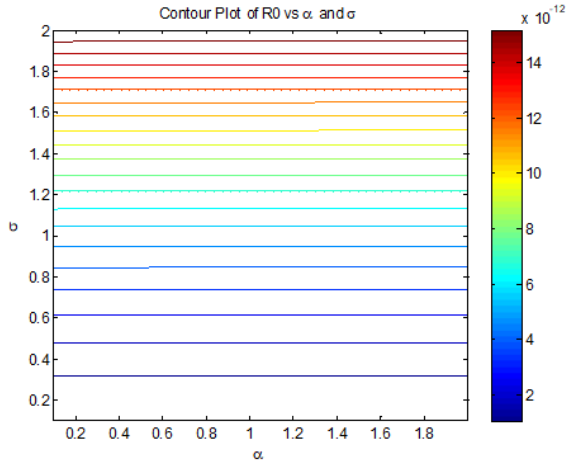

(a) contour plot showing the Impact of α and σ on R_0^d

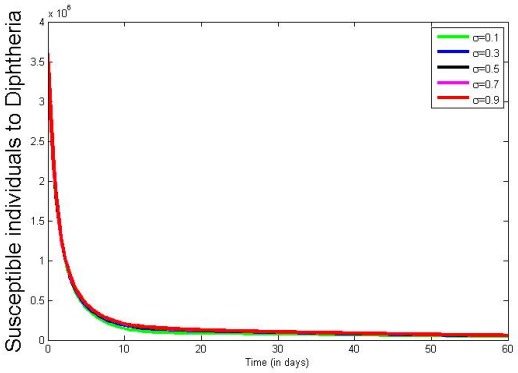

(b) Simulation of Susceptible individuals to Diphtheria

Figure 5: Contour plot on Impact of α and σ on R_0^d and Effect of σ on $S_d(t)$

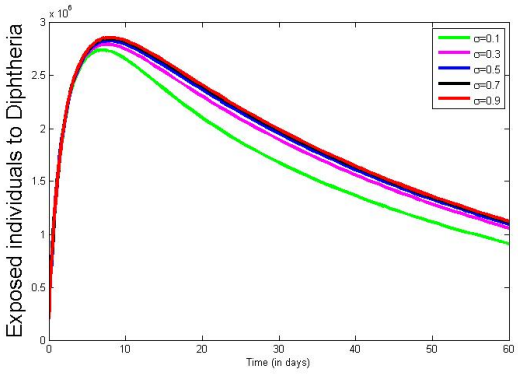

(a) Simulation of Exposed individuals to Diphtheria

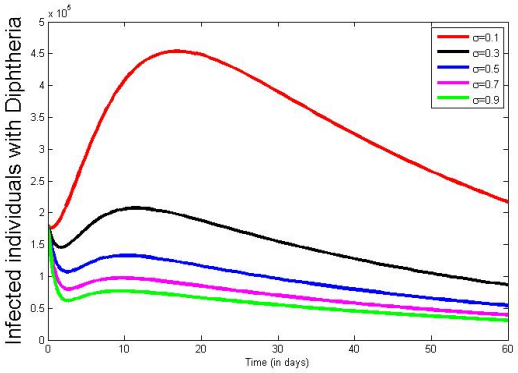

(b) Simulation of Infected individuals with Diphtheria

Figure 6: Effect of σ on $E_d(t)$ and $I_d(t)$

Figure 6(b) illustrates the dynamics of the infected human population over time. Initially, the number of infected individuals increases due to the influx from the exposed class. However, at a certain point, the number of infected individuals begins to decrease due to treatment interventions. This suggests that utilizing treatment and vaccination strategies will ultimately reduce the burden of diphtheria within the population. Figure 7(a) shows how the number of individuals receiving treatment changes over time. Initially, there is an increase in the treated population due to transfers from the infected group. Later, the number of individuals undergoing treatment gradually declines as successful medical interventions lead to recovery from diphtheria. Figure 7(b) shows that the vaccinated segment of the population initially increases as people follow vaccination protocols to prevent diphtheria. However, this population later decreases due to the declining effectiveness of the diphtheria vaccine over time, due to its inherent imperfections. Figure 8(a) shows an increase in the infected human population due to the presence of bacteria in the environment. Additionally, Figure 8(b) shows an increase in the recovered human population as the treatment rate rises. This is due to the effectiveness of the treatment strategies implemented by healthcare providers. This highlights the importance

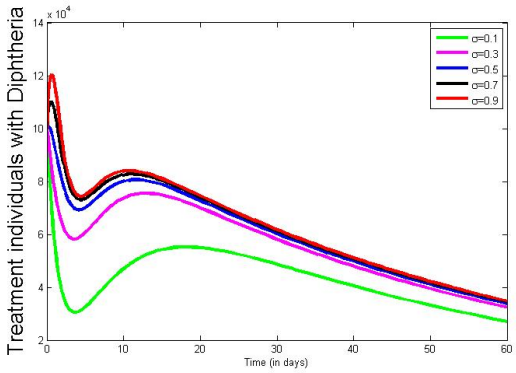

(a) **Simulation of Treatment individuals with Diphtheria**

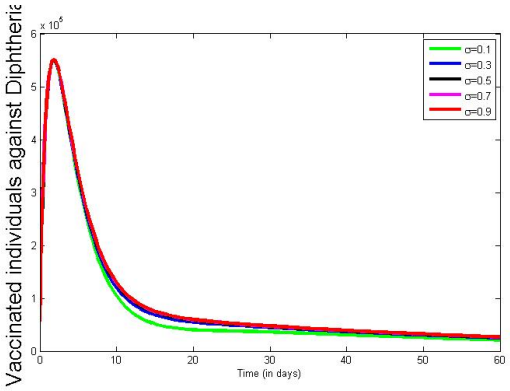

(b) **(b) Simulation of Vaccination individuals against Diphtheria**

Figure 7: **Effect of σ on $T_d(t)$ and $V_d(t)$**

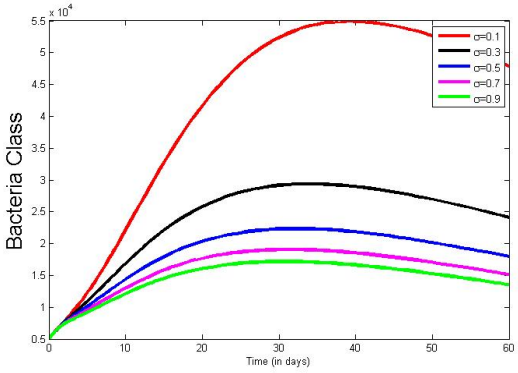

(a) **Simulation of the Bacteria class**

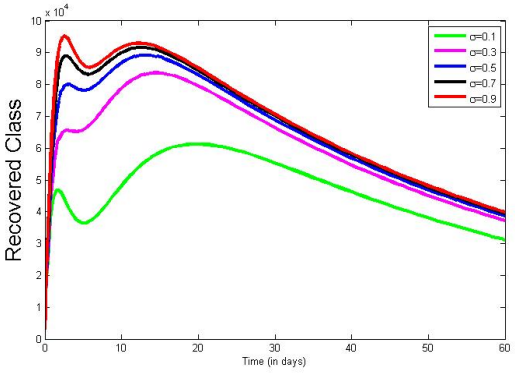

(b) **(b) Simulation of Recovered individuals from Diphtheria**

Figure 8: **Effect of σ on $B(t)$ and $R_d(t)$**

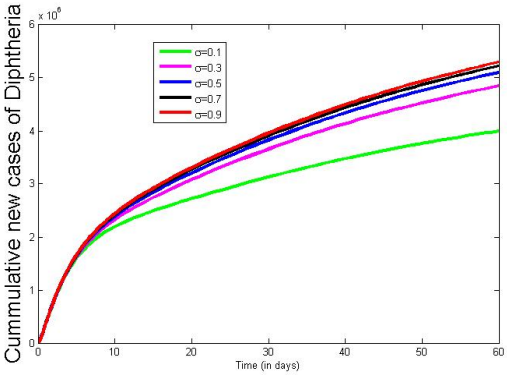

(a) **Cumulative new cases of Diphtheria**

Figure 9: **Effect of σ on the Cumulative new cases of Diphtheria**

of establishing diphtheria treatment facilities by government authorities to help reduce the prevalence of the disease in the population. Figure (9) shows an increase in the cumulative number of new diphtheria cases as the treatment rate between susceptible and infected individuals increases. The graph indicates that increasing the treatment rate leads to a reduction in the cumulative new cases of diphtheria, ultimately reducing the burden and prevalence of

the disease within the population.

5 Conclusion

This manuscript presents a mathematical model for the transmission dynamics and control of diphtheria using the Caputo fractional derivative. Initially, we developed an integer-order nonlinear system with seven differential equations, dividing the human population into six subgroups and including a separate bacteria class, resulting in a total of seven compartments. Acknowledging the importance of fractional modeling, we extended the integer-order model to fractional order using the Caputo operator. We began with a comprehensive theoretical analysis of the fractional diphtheria model, covering aspects such as solution existence, uniqueness, and equilibrium stability. We carried out the sensitivity analysis of the basic reproduction and is observed that the parameters like ϕ modification parameter that accounts for diphtheria induced death, rate at which susceptible individuals are vaccinated α, rate of treatment σ, the rate at which individuals under treatment recovered ε, disease induced death rate δ , natural death rate μ and bacteria natural death rate μ_B are with negative sensitivity indices and will reduces the prevalence of diphtheria within the humans population. Using the fractional Adams–Bashforth–Moulton method, we numerically solved the fractional model. The simulations visually demonstrated the impact of the disease incidence based on different model parameter values and fractional orders of the Caputo operator. Additionally, we conducted simulations by adjusting parameters such as the treatment rate for infected individuals, the vaccination rate for susceptible individuals, the contact rate between susceptible and infected individuals, the progression rate from exposed to infected, and the waning rate of the vaccine. The results indicated that enhancing treatment and vaccination strategies will effectively reduce the prevalence of diphtheria among the population. The study of novel trial functions and rogue waves in generalized breaking soliton equations using the bilinear neural network method, as presented by [29], suggests that this method could also be applied to solve nonlinear partial differential equations in future work.

Funding
There is no financing available.

Conflict of interest
The authors declare that they have no known competing interests.

Author's contribution
Emmanuel Abah: Formulating the model, concept, devising methodology.
Bolarinwa Bolaji: Authoring the final draft of the manuscript, creating visualization and providing supervision.
Godwin Onuche Acheneje: Authoring the initial draft of the manuscript, partaking in reviewing and editing process for the draft manuscript.
William Atokolo: partaking in reviewing and editing process for the draft manuscript.
Benjamin Idoko Omede: Partook in authoring the initial draft of the manuscript, reviewing and editing process for the draft manuscript.
Jeremiah Amos: partaking in reviewing and editing process for the draft manuscript.
Daniel Omeje: partaking in editing process for the draft manuscript.

All authors read through the manuscript and approved submission for publication.

Availability of data

The sources of all the data used in this work are variously cited in the literature.

References

[1] Todar, K. (2008). Diphtheria. University of Wisconsin-Madison Department of Bacteriology, 1-8.

[2] Singh, J., Harit, A. K., Jain, D. C., Panda, R. C., Tewari, K. N., and Bhatia, R. (1999). Diphtheria is declining but continues to kill many children: Analysis of data from a sentinel center in Delhi. Epidemiology and Infection, 123, 209-215.

[3] Galazka, A. M., and Robertson, S. E. (1995). Diphtheria: Changing patterns in the developing world and the industrialized world. European Journal of Epidemiology, 11, 107-117.

[4] Cárdenas, R., Prieto, G., Vargas, J., and Martinez, A. (1972). Corynebacterium diphtheriae. Características de cepas aisladas recientemente en Maracaibo - Venezuela. Kasmera, 4, 185-198.

[5] Formiga, L. C. D. (1985). New possibilities for the laboratory diagnosis of diphtheria. Brazilian Journal of Medical and Biological Research, 18, 401-402.

[6] Kneen, R., Phan, N. G., Solomon, T., Tran, T. M., Nguyen, T. T., Tran, B. L., Wain, J., Day, N. P., Tran, T. H., Parry, C. M., and White, N. J. (1998). Penicillin vs erythromycin in the treatment of diphtheria. Clinical Infectious Diseases, 27, 845-850.

[7] Bachran, C., Sutherland, M., Bachran, D., and Fuchs, H. (2007). Quantification of diphtheria toxin-mediated ADP-ribosylation in a solid-phase assay. Clinical Chemistry, 53(9), 1676-1683.

[8] Brooks, G. F., Carroll, C. K., Butel, J. S., and Morse, A. S. (2007). Jawetz, Melnick and Adelberg's Medical Microbiology (24th ed., pp. 154-217).

[9] Formiga, L. C. D., and Mattos-Guaraldi, A. L. (1993). Diphtheria: Current status and laboratory procedures for diagnosis. Revista Brasileira de Patologia Clínica, 29, 93-96.

[10] Atokolo, W., Aja, R. O., Aniaku, S. E., Onah, I. S., and Mbah, G. C. E. (2022). Approximate solution of the fractional order sterile insect technology model via the Laplace–Adomian decomposition method for the spread of Zika virus disease. International Journal of Mathematics and Mathematical Sciences, 2022, 1–24. https://doi.org/10.1155/2022/2297630

[11] Atokolo, W., Aja, R. O., Omale, D., Ahman, Q. O., Acheneje, G. O., and Amos, J. (2024). Fractional mathematical model for the transmission dynamics and control of Lassa fever. Franklin Open, 100110. https://doi.org/10.1016/j.fraope.2024.100110

[12] Agahiu, N., Bolaji, B., and Atokolo, W. (2024). Approximate solution of fractional order mathematical model on the co-transmission of zika and chikungunya virus using laplace adomian decomposition method. GPH-International Journal of Mathematics, 7(03), 47-81.

[13] Odionyenma, U. B., Ikenna, N., and Bolaji, B. (2023). Analysis of a model to control the co-dynamics of Chlamydia and Gonorrhea using Caputo fractional derivative.

Mathematical Modelling and Numerical Simulation With Applications, 3(2), 111–140. https://doi.org/10.53391/mmnsa.1320175

[14] Zhang, Z., Zeb, A., Egbelowo, O. F., and Erturk, V. S. (2020). Dynamics of a fractional order mathematical model for COVID-19 epidemic. Advances in Difference Equations, 2020(1).https://doi.org/10.1186/s13662-020-02873-w

[15] Ghani, M., Utami, I. Q., Triyayuda, F. W., and Afifah, M. (2022). A fractional SEIQR model on diphtheria disease. Modeling Earth Systems and Environment, 9(2), 2199–2219. https://doi.org/10.1007/s40808-022-01615-z

[16] Mangal, S., Misra, O. P., and Dhar, J. (2023). Modeling the effect of vaccination in fractional-order epidemic model for infectious disease. International Journal of Dynamics and Control, 12(1), 303–317. https://doi.org/10.1007/s40435-023-01331-1

[17] Rajan, P. K., Kuppusamy, M., and Yusuf, A. (2023). A fractional-order modeling of human papillomavirus transmission and cervical cancer. Modeling Earth Systems and Environment, 10(1), 1337–1357. https://doi.org/10.1007/s40808-023-01843-x

[18] Yunus, A. O. and Olayiwola, M. O. (2024). The analysis of a novel covid-19 model with the fractional-order incorporating the impact of the vaccination campaign in nigeria via the laplace-adomian decomposition method. Journal of the Nigerian Society of Physical Sciences, 1830. https://doi.org/10.46481/jnsps.2024.1830

[19] Akogwu, B. (2022). The solution of a mathematical model for COVID-19 transmission and vaccination in Nigeria by using a differential transformation method. FUDMA Journal of Sciences, 6(5), 50-56. https://doi.org/10.33003/fjs-2022-0605-1089

[20] Milici, C., Draganescu, G., and Machado, J. T. (2018). Introduction to fractional differential equations. Springer.

[21] Podlubny, I. (1998). Fractional differential equations: An introduction to fractional derivatives, to methods of their solution and some of their applications. Elsevier.

[22] VandenDriessche, P. and Watmough, J. (2002). Reproduction numbers and subthreshold endemic equilibria for compartmental models of disease transmission. Mathematical Biosciences, 180(1-2), 29-48.

[23] Zhang, R. and Li, M. (2022). Bilinear residual network method for solving the exactly explicit solutions of nonlinear evolution equations. Nonlinear Dynamics, 108. http://dx.doi.org/10.1007/s11071-022-07207-x

[24] Baskonus, H. M. and Bulut, H. (2015). On the numerical solutions of some fractional ordinary differential equations by fractional adams bashforth-moulton method. Open Mathematics, 13, 1.

[25] Diethelm, K. (1999). The FracPECE subroutine for the numerical solution of differential equations of fractional order. Open Mathematics, 13, 1.

[26] Puspita, G., Kharis, M., and Supriyono. (2017). UNNES Journal of Mathematics, 6, 25-3.

[27] Fathoni, M. I., Mardlijah, and Hariyanto. (2015). Proceedings of the national seminar on mathematics and mathematics education. Proceedings of the National Seminar on Mathematics and Mathematics Education, 229–238.

[28] Ministry of National Development Planning (MNDP), Central Bureau of Statistics Indonesia, and United Nations Population Fund (UNFPA) Indonesia. (2013). Indonesia population projection 2010-2035 (pp. 34, 84-468). BPS-Statistic Indonesia.

[29] Zhang, R. F., Li, M.-C., Gan, J. Y., Li, Q., and Lan, Z.-Z. (2022). Novel trial functions and rogue waves of generalized breaking soliton equation via bilinear neural network method. Chaos, Solitons & Fractals, 154. https://doi.org/10.1016/j.chaos.2021.111579